

# Enumerating combinatorial triangulations of the hexahedron

Jeanne Pellerin\* and Jean-François Remacle †

## Abstract

Most indirect hexahedral meshing methods rely on 10 patterns of subdivision of the hexahedron into tetrahedra. A recent observation at least one more pattern exists raise the question of the actual number of subdivisions of the hexahedron into tetrahedra. In this article answers we enumerate these subdivisions by exhausting all possible ways to combine tetrahedra into hexahedra. We introduce a combinatorial algorithm that (1) generates all the combinations of tetrahedra that can be built from eight vertices and (2) tests if they subdivide a hexahedron or not. The challenge is that there are  $2^{70}$  combinations of tetrahedra to consider. We use topological arguments and an efficient pruning strategy to drastically reduce this number. Our main result is that there are 6,966 combinatorial triangulations of the hexahedron which can be classified into 174 equivalence classes. Our results are consistent with theoretical results available on the subdivision of the cube.

**Keywords:** combination, tetrahedra, meshing, graph, isomorphism

## 1 Introduction

In this paper we propose an algorithm to combinatorially enumerate the subdivisions of a hexahedron into tetrahedra. This work is motivated by recent papers proposing to generate meshes based on the combination of tetrahedra into a hexahedron. The initial method applying that approach was proposed by [Meshkat and Talmor \(2000\)](#). It is based on a set of 6 predefined patterns of subdivision of a hexahedron into tetrahedra and searches for their occurrences in the input tetrahedral mesh. Used by [Levy and Liu \(2010\)](#) and [Huang et al. \(2011\)](#), it was further extended by [Botella et al. \(2016\)](#) and [Sokolov et al. \(2016\)](#) to operate with 10 patterns. An alternative strategy was proposed by [Yamakawa and Shimada \(2003\)](#), it is based on the vertices of the mesh and was used by [Baudouin et al. \(2014\)](#) and further generalized by [Pellerin et al. \(2017\)](#). This last method does not depend on any pattern of subdivision of the hexahedron into tetrahedra. [Pellerin et al. \(2017\)](#) obtained unexpected results and observe some hexahedra correspond to subdivision patterns unaccounted for in previous works. They exhibit a configuration with eight tetrahedra which is a counter example to the theorem of [Sokolov et al. \(2016\)](#) that the hexahedron has subdivisions into 5, 6, or 7 tetrahedra. These recent results raise the question tackled in this paper: How many triangulations of the hexahedron do exist? In the particular case of the cube, the answer is 74 and 6 of them are different up to the relabeling of their vertices ([De Loera et al., 2010](#)). We consider a more general hexahedron, that can be defined combinatorially as a 3-manifold homeomorphic to

---

\*Université catholique de Louvain, [jeanne.pellerin@uclouvain.be](mailto:jeanne.pellerin@uclouvain.be)

†Université catholique de Louvain, [jean-francois.remacle@uclouvain.be](mailto:jean-francois.remacle@uclouvain.be)

a 3-ball that has exactly 8 vertices and which boundary matches the triangulated boundary of a cuboid.

In this paper, we exhaust all possible ways to combine tetrahedra into hexahedra. In other words, we enumerate the combinatorial triangulations of the hexahedron. Our algorithm generates all the combinations of the  $\binom{8}{4} = 70$  tetrahedra that can be built from 8 vertices and tests each combination of tetrahedra to determine if it is a valid combinatorial triangulation of the hexahedron. A naive implementation would be inefficient because (i) the number of combinations to consider is  $2^{70}$  (ii) many subdivisions are isomorphic, i.e. they are the same up the relabeling of their vertices. After an aggressive optimization and parallelization the final algorithm runs in a few hours. Our main result is that there are 6,966 triangulations of the hexahedron. To compare triangulations and compute those similar up to the relabeling of their vertices we use the formalism of [Meshkat and Talmor \(2000\)](#). We enumerate 174 isomorphism-free triangulations of the hexahedron with 5 to 15 tetrahedra.

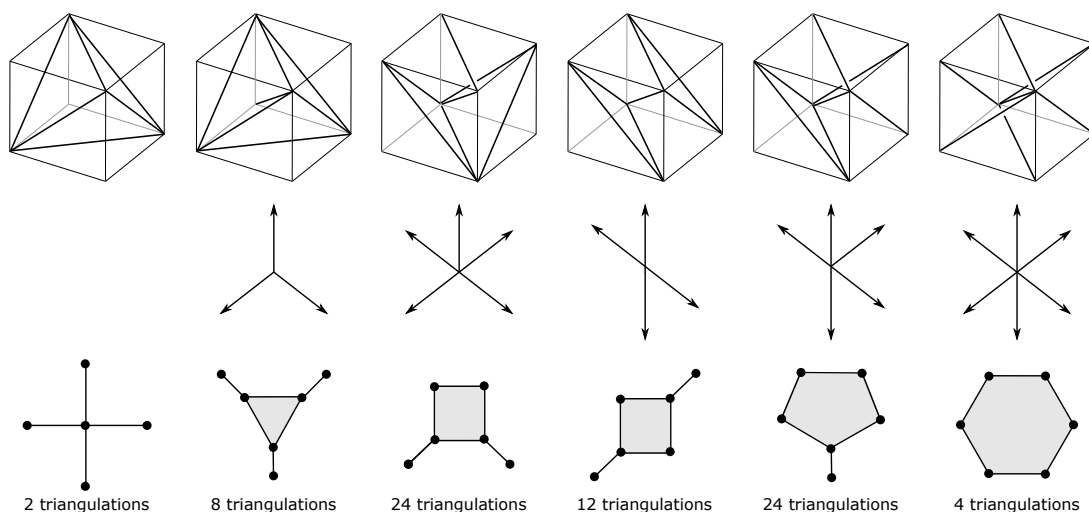


Figure 1: The six types of triangulations of the 3-cube  $I^3 = [0, 1]^3$ , their link at the diameter edge and their dual complexes.

We further examine which of the 174 triangulations correspond to a valid geometrically triangulation in  $\mathbb{R}^3$ . By valid geometrical triangulation, we mean a triangulation in which all tetrahedra have a strictly positive volume. We implemented the algorithm of [Pellerin et al. \(2017\)](#) and applied it on the Delaunay triangulations of randomly generated points.

## 2 Related work

A triangulation of a hexahedron is a subdivision of the interior of the hexahedron into a set of conformal tetrahedra without any additional vertex. The tetrahedra induce a subdivision of each facet into two triangles. We say that a triangulation is geometrically valid if all its tetrahedra have a strictly positive volume.

## 2.1 Triangulations of the cube

In this section, we review results on the triangulations of the cube.

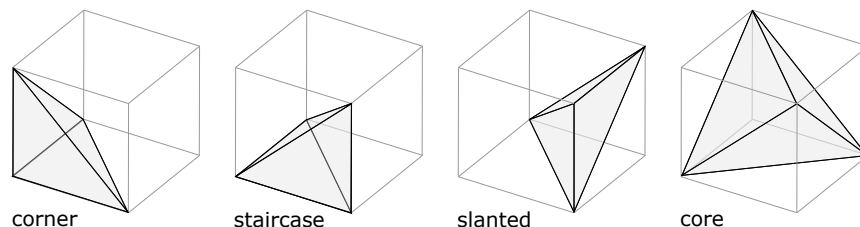


Figure 2: The four types of tetrahedra in a cube have three, two, one or no facet on the hexahedron boundary.

**The cube** Following [De Loera et al. \(2010\)](#), let us first look at the different types of tetrahedra that can be built from the eight vertices of a cube  $I^3 = [0, 1]^3$ . Modulo cube symmetries there are four types of tetrahedra:

- Corner tetrahedra are obtained from a vertex together with its three neighbors, they have three facets on the hexahedron boundary.
- Staircase tetrahedra are obtained from vertices forming a monotone path between opposite vertices of the cube, they have two facets on the hexahedron boundary.
- Slanted tetrahedra are obtained from two opposite vertices and two neighbors of one of them, they have one facet on the hexahedron boundary.
- Core tetrahedra are obtained from two sets of diagonally opposite vertices, they have no facet on the hexahedron boundary.

For the 3-cube, this list is complete and irredundant ([De Loera et al., 2010](#)). From this classification of the tetrahedra in a cube triangulation follows the classification of triangulations of the 3-cube. The 3-cube has exactly 74 triangulations that are classified in 6 classes (see ([De Loera et al., 2010](#)) and references therein).

- Every triangulation of the 3-cube contains either a regular tetrahedron (i.e. a tetrahedron whose 6 edges are of equal lengths) or a diameter, i.e. an interior edge joining two opposite vertices.
- There are two triangulations of the first type, symmetric to one another. The triangulations of the second type are completely classified, modulo symmetries, by their link at the diameter. The triangulations containing an interior edge are completely classified modulo symmetries by their link at the diameter.
- That link can be one of the five shown in [Figure 1](#) middle.

We recall here the link of the cube diameter edge is the set of vertices opposite to the edge in the triangle facets incident to this edge. More formally, the link of a simplex  $\sigma$  in a triangulation

$T$ , is  $link(\sigma) = \{\tau \in star(\sigma) | \sigma \cap \tau = \emptyset\}$ , where the star of  $\sigma$  the set of all simplices of  $T$  having  $\sigma$  as a face plus all their faces. Another way to visualize the six different types of triangulations of the 3-cube is their dual complexes (Figure 1 bottom). The dual complex is a graph in which there is a vertex for each tetrahedron and one edge if corresponding tetrahedra share a triangle. By construction, a 2-cell of the dual complex corresponds to an interior edge of the triangulation.

There are at least two main ways to prove that these six triangulations are indeed the six possible types of triangulations of the cube. Discrete geometers relies on the determination of the cell containing the barycenter of the cube and on symmetry considerations about the link of that cell (De Loera et al., 2010) while Meshkat and Talmor (2000) enumerate the possible dual complexes.

**The 3-cube in finite precision** Computers floating point numbers have a finite precision and represent the cube  $I^3 = [0, 1]^3$  up to some tolerance. Moreover, cospherical and coplanar sets of points must often be specifically processed since they are not in general position, e.g. their Delaunay triangulation is not unique (Edelsbrunner and Mücke, 1990). Therefore, to combine elements of given tetrahedral meshes, Botella et al. (2016) and Sokolov et al. (2016) consider subdivisions of the cube into two prisms linked by a *sliver*, i.e. a very flat tetrahedra connecting four points that are coplanar up to a given tolerance.

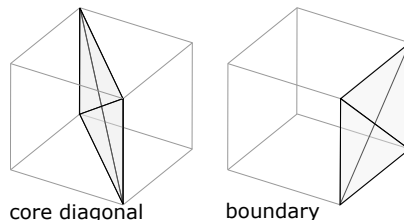


Figure 3: Two types of tetrahedra in an finite precision cube.

In a finite precision 3-cube, two new types of tetrahedra appear this way (Figure 3):

1. Core diagonal tetrahedra connect vertices of diagonally opposite edges. They have no facet on the hexahedron boundary, four hexahedron edges, and two interior edges. They divide the hexahedron into two prisms, creating four additional types of triangulations into seven tetrahedra (Figure 4).
2. Boundary tetrahedra connect the four vertices of a facet of the cube. They have two facet on the hexahedron boundary four hexahedron edges, one diagonal edge and one interior edge. Theoretically they could be added to any of the six cube faces, multiplying by  $2^6 = 64$  the number of triangulations of the cube. They are therefore ignored in the remaining of this paper.

Note that in the triangulation of a hexahedron into seven tetrahedra, the dual complex is not sufficient to represent different triangulations. The two triangulations left of Figure 4 have isomorphic dual complexes but are themselves not isomorphic. The difference lies in the quadrilateral facets: pairs of tetrahedra having a facet incident to the same quadrilateral facet change. This link is represented by dashes edge in the pattern graphs, a formalism introduced by Meshkat and Talmor (2000) that we use throughout this paper.

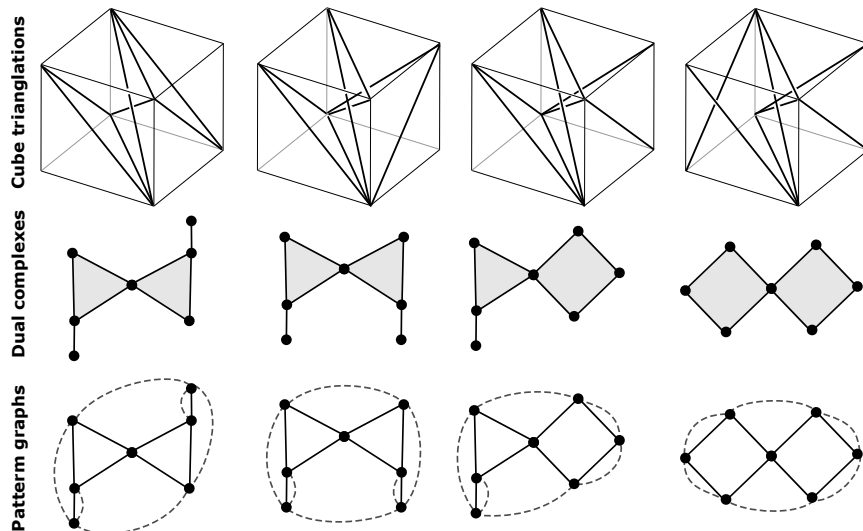


Figure 4: Four triangulations of a finite precision cube in seven tetrahedra.

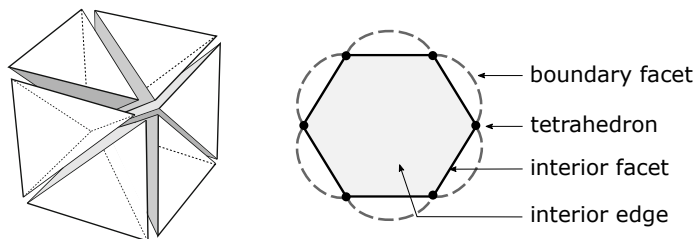


Figure 5: Decomposition pattern definition.

## 2.2 Decomposition graph

In this section we precise the formalism we will use throughout this paper to analyze and compare triangulations of hexahedra. This formalism was initially introduced by Meshkat and Talmor (2000).

The *decomposition pattern* (Figure 5) of the triangulation of a hexahedral cell is an edge colored graph where there is one vertex per tetrahedron, one black (plain) edge between vertices if the corresponding tetrahedra are adjacent, and one grey (dashed) edge between vertices if the corresponding tetrahedra have triangle faces on the same hexahedron facet. By construction, simple chordless cycles of plain edges correspond to interior edges of the triangulation. Moreover the dashed edges correspond to diagonal edges of the hexahedron triangulation. The tetrahedra sharing each diagonal edge can be deduced from graph cycles that contains exactly one dashed edge.

There is a one-to-one correspondence between triangulations without boundary tetrahedra and decomposition patterns. Indeed, if we fix the vertex labels of the triangulation so that  $\{12345678\}$  is a hexahedron, 12 edges are fixed. Choosing 6 diagonal facets, we fix the 12 boundary facets of the triangulation. The remaining degrees of freedom to triangulate the interior of the hexahedron are controlled by the interior facets. The set of tetrahedra is then fully determined.

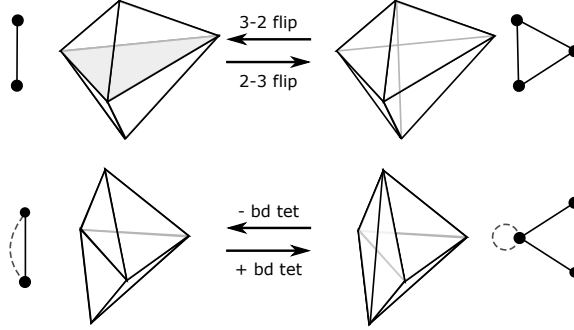


Figure 6: The two base operations on hex triangulations. Top: 2-3 flip. Bottom: addition of boundary tetrahedron.

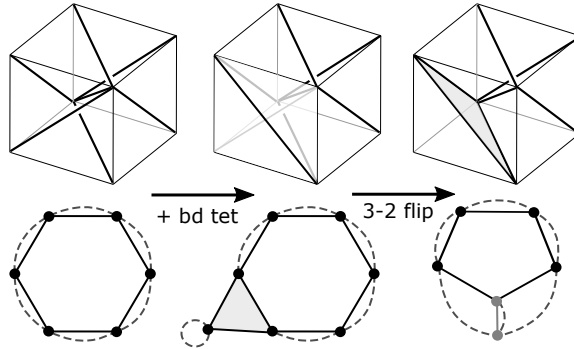


Figure 7: Face diagonal flip may be seen as the combination of two base operations.

Two hexahedron triangulations are *equivalent* if they are the same up to the relabeling of their vertices. They are then *equivalent* when their decomposition graphs are isomorphic, i.e. are the same with respect to the relabeling of their vertices. More formally, an isomorphism of graphs  $G$  and  $H$  is a bijection between the vertex sets of  $G$  and  $H$ ,  $f : V(G) \rightarrow V(H)$ , such that any two vertices  $u$  and  $v$  of  $G$  are adjacent if and only if  $f(u)$  and  $f(v)$  are adjacent in  $H$ .

**Operators on the decomposition graph** All triangulation modification operations can be translated in operations on the decomposition graph. The most important one is the 2-3 flip, i.e. an operation that replace one facet and the two incident tetrahedra by an edge and three tetrahedra incident to it (Figure 6-top). A 2-3 flip may be realized only if the edge intersect the facet. In all other cases, the edge is said non-flippable. The second operation is the addition of a boundary tetrahedron (Figure 6-bottom). This operation cannot be used alone since boundary tetrahedra are ignored in decomposition graphs. For example, it may be combined with a 3-2 flip to flip a face diagonals (Figure 7). Note that a boundary tetrahedron may be added only if the quadrilateral face is concave.

Using these two operations we can deduce all ten cube triangulations from the triangulation into five tetrahedra. We can also built other decomposition graphs. For example, adding a boundary tetrahedron to the five tetrahedron pattern and then performing a 2-3 flip, we obtain a decom-

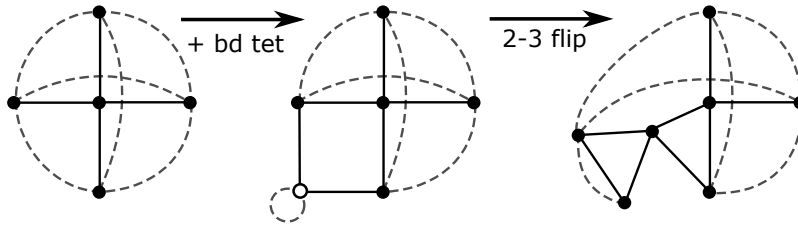


Figure 8: Seven tetrahedra decomposition graph built by modifying the cube decomposition in 5 tetrahedra.

position into 7 tetrahedra that is unaccounted for in previous works (Figure 8). As long as the geometrical conditions are met to allow the addition of the boundary tetrahedron and the edge flipping, these graph modifications will correspond to valid geometrical hexahedron triangulations.

### 3 Lexicographic enumeration

In this section, we enumerate all valid combinatorial triangulations of the hexahedral cell as well as their decomposition graphs.

#### 3.1 Hexahedron boundary triangulations

Testing if a combinatorial triangulation is a valid decomposition of hexahedron requires testing if the boundary of this triangulation is a valid hexahedron boundary. The triangulation of the boundary of a hexahedron has 8 vertices and 18 edges. Among these, 12 are fixed and there are 2 possibilities to place the remaining 6 diagonals of the quadrilateral facets. We have then  $2^6 = 64$  possible triangulations. They can be classified into 7 equivalency classes, each one corresponding to non-isomorphic triangulations of the hexahedron boundary (Figure 9). Depending on their symmetries they correspond to 2 to 24 triangulations of a hexahedron boundary.

Two triangulations of the boundary of the hexahedron (F and G) contain one set of cyclic diagonals. According to Rambau (2003)'s theorem, the 3-cube does not admit any triangulation that uses cyclic diagonals. However, the finite precision cube does since one decomposition into seven tetrahedra (right on Figure 4) matches F, and, as we will see in Section 4, other subdivisions match G.

#### 3.2 Lexicographic enumeration of the hexahedron triangulations

We now exhaust all valid combinatorial triangulations of the hexahedral cell. Our strategy is to (i) generate all possible combinations of tetrahedra defined of 8 vertices, then (ii) test whether or not they are valid triangulations of the hexahedron, and finally (iii) compare decomposition graphs testing their isomorphism with nauty (<http://pallini.di.uniroma1.it/>) (McKay and Piperno, 2014).

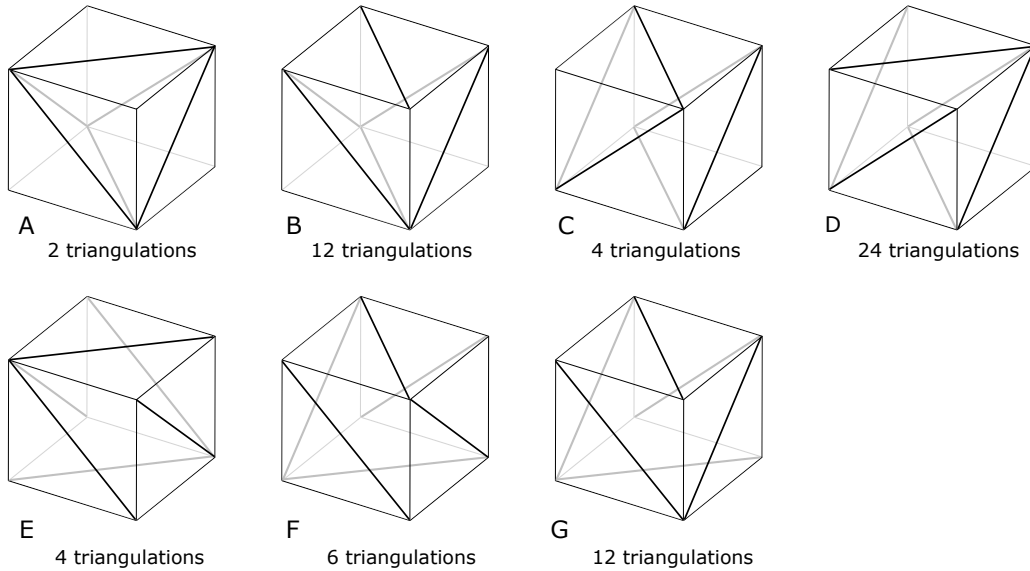


Figure 9: The 7 isomorphism free triangulations of a hexahedron boundary.

### 3.2.1 Definitions and naive implementation

We consider the hexahedron  $\{12345678\}$ , its 12 edges are  $\{12\}, \{14\}, \{15\}, \{23\}, \{26\}, \{34\}, \{36\}, \{48\}, \{56\}, \{58\}, \{67\}, \{78\}$  and its 6 facets are  $\{1234\}, \{1265\}, \{1485\}, \{2376\}, \{3487\}, \{5678\}$ . The objective is to enumerate all triangulations of this hexahedron and to classify them into isomorphism-free classes. We are going to generate all sets of tetrahedra, facets, edges that can be defined from 8 vertices, i.e. choose among:

- $\binom{8}{1} = 8$  vertices ( $\{1\}, \{2\}, \dots, \{8\}$ ),
- $\binom{8}{2} = 28$  edges ( $\{12\}, \{13\}, \dots, \{78\}$ ),
- $\binom{8}{3} = 56$  facets ( $\{123\}, \{124\}, \dots, \{678\}$ ),
- $\binom{8}{4} = 70$  tetrahedra ( $\{1234\}, \{1235\}, \dots, \{5678\}$ ).

The set of facets, edges, and vertices of a triangulation can be deduced from the choice of tetrahedra. There are as many combinations as there are subsets of 70 tetrahedra, i.e.  $2^{70}$  combinations to test. Topological arguments give that the hexahedron triangulation has between 5 and 15 tetrahedra. The topology of the boundary is fixed to 8 vertices, 12 facets and 18 edges. Each tetrahedron has 4 facets, each interior is incident to 2 tetrahedra, then  $4t = 2f + 12$ . Injecting this in the Euler-Poincaré characteristic of the triangulation  $\chi = v - e + f - t = 1$ , we have  $t = e - 13$ . There are at least 18 boundary edges and at most  $\binom{8}{2} = 28$  edges in the triangulation of a hexahedron, then  $5 \leq t \leq 15$  (see [Edelsbrunner et al. \(1990\)](#) for more combinatorial results). This reduces the sets of tetrahedra to test to all  $k \in [5; 15]$  combinations among  $n = 70$  tetrahedra.

A set of tetrahedra is a valid combinatorial triangulation of the hexahedron if it is a valid combinatorial 3-manifold which boundary matches one of the seven possible hexahedron boundary



---

**Algorithm 1:** Naive enumeration of all hexahedron combinatorial triangulations.

---

```
1 foreach  $k \in [5; 15]$  do
2   /* Initialize the combination of tetrahedra */
3   combination = {-1, 1, 2, .., k} ;
4   local j = k ;
5   done = false;
6   while ! done do
7     if isValid(combination) then store(combination);
8     /* Next combination in lexicographic order */
9     combination[j] = combination[j] +1;
10    foreach  $i \in [j + 1; k]$  do combination[i] = combination[i-1]+1;
11    if  $j \neq 0$  then done = true;
12    else
13      if combination [k] < 70 then j = k;
14      else j = j-1;
15      done = false;
```

---

triangulation computed in Section 3.1. We can test combinatorially that the triangulation is a manifold by testing that the links of all vertices are triangulated 2-half-spheres. (see Section 2.1 for the link definition). We can use graph isomorphism tests to ensure that the boundary is valid.

Algorithm 1 follows, it enumerates isomorphism-free triangulations of the hexahedron {12345678}. All combinations of 5 to 15 tetrahedra among 70 are generated by an incremental lexicographic algorithm (Ruskey, 2003), then it tests if they are a valid triangulation of the hexahedron {12345678} and compare their decomposition graphs to previously identified ones.

### 3.2.2 Optimized implementation

The very large number of combinations of  $\binom{70}{k} : k \in [5; 15]$  makes the previously described algorithm unpractical for more than 7 tetrahedra. To be able to run the code in a reasonable amount of time for all numbers of tetrahedra, optimization of the validity test, a strategy to prune invalid combinations and parallelization of the code are implemented.

**Validity test** The validity test is performed billions of times and must be the most efficient possible. Sets of tetrahedra that are not hexahedron triangulations should be discarded as early as possible at the lowest possible computational cost. For a triangulation  $t$ , subset of the  $\binom{70}{k}$  possible tetrahedra, the following verifications are performed in this order,  $t$  should have:

1. 12 facets incident to one tetrahedron
2. No facet incident to more than 2 tetrahedra
3. 8 vertices
4. A Euler-Poincaré characteristic equal to 1
5. A connected manifold boundary without boundary (all edges are incident to two facets).

---

**Algorithm 2:** Optimized enumeration of all triangulations of the hexahedron with  $k$  tetrahedra.

---

```

Data:  $n = 70$ ,  $k \in [5;15]$ , firstCombination, lastCombination
1 combination  $\leftarrow$  firstCombination;
2 local  $j = k$  ;
3 while  $j \neq 0$  and combination  $<$  lastCombination do
4   if isValidTriangulation(combination) then storeTetCombination(combination);
5   /* Remove values right of j                                     */
6   removeTets( $j+1$ ,  $k$ ) ;
7   /* Move j to the left as long as we have to                       */
8   moveLeftRemoveTets[j];
9   /* Increment j value                                           */
10  incrementTet[j];
11  while  $j \neq 0$  do
12    if invalidNumbersFacets( $k$ ,  $j$ ) then
13      /* Pruning                                                  */
14      moveLeftRemoveTets[j];
15      incrementTet[j];
16    else if  $j < k$  then
17      /* Complete the combination                                 */
18       $j = j+1$ ;
19      addTet( $j$ , combination [ $j-1$ ]+1);
20    else
21      /* Set next rightmost changeable position                 */
22      while  $j \neq 0$  and combination[j] ==  $n-k+j$  do  $j=j-1$ ;
23      break ;

```

---

6. The 12 edges of hexahedron {12345678} and 6 face diagonal edges.
7. All tetrahedra incident to a vertex are connected.
8. No boundary tetrahedron, i.e. no tetrahedron with 4 vertices in the same hexahedron facet (Figure 3).

This order is the optimal one to discard invalid combinations of tetrahedra as early as possible. It takes into account the number of combinations rejected, the relative dependency of the tests and their cost. To minimize the computational cost of the first four tests, arrays tracking the number of times each of the 70 tetrahedra, 56 facets, 28 edges, and 8 vertices appears in the current tetrahedron combination are updated when a combination value is modified. Numbers of invalid facets (incident to 3 or more tetrahedra), boundary facets (incident to 1 tetrahedra), interior facets (incident to 2 tetrahedra) are also maintained.

**Pruning combinations with invalid facet number** The great majority of combinations of tetrahedra are discarded by the first two validity tests, i.e. they do not have 12 boundary facets and/or at least one invalid facet. The objective here is to skip generating such combinations. In Algorithm 1, the combinations of  $k$  tets are iteratively generated in a lexicographical order. At each step, the combination value at the rightmost changeable position  $j$  is incremented till maximal value  $n - k + j$ . But, if the first  $(j - 1)$  elements of the combination define an invalid facet,  $j$  may be decreased without testing these combinations. Similarly, if the first  $(j - 1)$  elements define a number of boundary facets that cannot be altered to reach 12 by adding the next  $k - j$  tetrahedra, the following combinations are not valid. The first  $(j - 1)$  elements should then have a number of boundary facets between  $12 + 4(k - j)$  and  $12 + 4(k - j) - 4(k - j)$ ,  $4(k - j)$  being the maximal number of boundary facets added or removed when adding the missing tetrahedra to the combination. The optimized Algorithm 2 skips all the combinations that do not have 12 boundary facets, or an invalid facet.

**Parallelization** To divide the workload between threads, we use combination ranks to split the number of combinations into  $m$  parts that are processed in parallel. The rank of a combination is the position (positive integer) that the combination occupies in the ordering imposed by the generation algorithm, here it is lexicographic. For combinations of  $k$  tetrahedra, the rank of the first combination in part  $j \in [0; m - 1]$  is  $R_j = \frac{j}{m} \binom{70}{k}$ , the rank of the last combination being  $R_{j+1} - 1 = \frac{j+1}{m} \binom{70}{k} - 1$ . To initialize consistently the incremental combination algorithm for each thread, first and last combinations to process are determined by unranking  $R_j$  and  $R_{j+1}$ .

### 3.3 Combinatorial results

Algorithm 2 has been executed on a 32 core Intel Xeon E5-4610 v2 @ 2.30GHz with 128 GB of memory to enumerate all combinatorial triangulations of the hexahedron {12345678}. Their decomposition graphs are subsequently grouped by pattern, i.e. isomorphism classes, using nauty library McKay and Piperno (2014). Results are obtained in less than a second for low numbers of tetrahedra and require a few hours for 14 and 15 tetrahedra. The complete enumeration runs in less than 9 hours. We count 6,966 triangulations of the hexahedron that are divided into 174 isomorphism classes. Details in terms of numbers of valid triangulations, numbers of patterns, and timings are given in Table 1. The decomposition graphs for the 174 classes are given on Figures 10

Table 1: Number of combinatorial triangulations of the hexahedron. Timings are given for a 32 core Intel Xeon E5-4610 v2 @ 2.30GHz machine.

#Tets	#Tet combinations	#Triangulations	#Patterns	Timing(s)	Figure
5	12,103,014	2	1	0.08	Fig. 10
6	131,115,985	72	5	0.31	Fig. 11
7	1,198,774,720	132	5	1.65	Fig. 12
8	9,440,350,920	312	7	10.24	Fig. 13
9	65,033,528,560	552	13	46.64	Fig. 14
10	396,704,524,216	852	20	194.26	Fig. 15
11	2,163,842,859,360	1,396	35	441.24	Fig. 16
12	10,638,894,058,520	1,348	30	1336.86	Fig. 17
13	47,465,835,030,320	1,164	28	3577.87	Fig. 18
14	193,253,756,909,160	840	19	8427.42	Fig. 19
15	721,480,692,460,864	296	11	16961.2	Fig. 20
Total	975,475,541,715,639	6,966	174	30997.78	

to 20. Each isomorphism class is given a name composed of the number of tetrahedra in the triangulation and one or two letters. Each isomorphism class corresponds to 2, 4, 8, 12, 16, 24, or 48 equivalent triangulations (Table 2).

**Consistency with cube triangulations** Our results are consistent with the classification of the 74 triangulations of the 3-cube. We obtain the exact same graphs and the same number of triangulations, i.e. 2 triangulations with 5 tetrahedra, and 72 triangulations with 6 tetrahedra (Figure 11). Our results are also consistent with the seven tetrahedron patterns used in pattern-matching methods for indirect hexahedral dominant meshing (Botella et al., 2016; Sokolov et al., 2016). We additionally obtain the number of triangulations corresponding to these four patterns. Note that we obtain a fifth decomposition graph into seven tetrahedra (Figure 12A) that is the graph we built on Figure 8.

This enumeration of all possible decomposition graphs is purely topological and does account for geometry. In the following we tackle the question of enumerating the possible valid geometrical triangulations of the hexahedron.

## 4 Geometrical realizations in $\mathbb{R}^3$

**Challenge** When enumerating all possible decomposition graphs by exhausting all possible decompositions into 5 to 15 tetrahedra of a hexahedron as proposed in Section 3, there is no guarantee that a valid geometrical triangulation exist for a pattern. If the realizability of a combinatorial triangulation (abstract simplicial complex) is guaranteed in a space of a big enough dimension, it is not in  $\mathbb{R}^3$ . By valid geometrical triangulation, we mean a triangulation in which all tetrahedra have a strictly positive volume. Two questions arise (i) which decomposition patterns correspond to a valid triangulation of eight vertices which positions are given? (ii) which of the decomposition graphs correspond to a valid geometrical triangulation? Since we do know all the possible triangulations that may define a hexahedron, we may test the validity of each for given points and answer the first question. The second question is more challenging. To prove that a decomposition pattern is realizable, it is sufficient to exhibit one realization, however proving the contrary is more difficult



Table 3: Number of different decomposition graphs counted in the Delaunay triangulations of random point sets of increasing size.

#vertices	5	6	7	8	9	10	11	12	13	14	15	Total
3,000	1	5	2	7	13	16	4	0	0	0	0	51
10,000	1	5	5	7	13	19	10	2	0	0	0	62
20,000	1	5	5	7	13	19	15	2	0	0	0	67
100,000	1	5	5	7	13	20	24	5	0	0	0	80
500,000	1	5	5	7	13	20	28	12	1	0	0	92
1,000,000	1	5	5	7	13	20	30	14	0	0	0	95
2,000,000	1	5	5	7	13	20	30	15	4	1	0	101
5,000,000	1	5	5	7	13	20	30	16	4	1	0	102
10,000,000	1	5	5	7	13	20	31	16	6	1	0	105
<i>Theoretical max.</i>	<i>1</i>	<i>5</i>	<i>5</i>	<i>7</i>	<i>13</i>	<i>20</i>	<i>35</i>	<i>30</i>	<i>28</i>	<i>19</i>	<i>11</i>	<i>174</i>

is restricted to the case where the considered hexahedra are cubes.

This study also provide tools to explore the boundary between triangulable and non-triangulable hexahedra. This is known as a very challenging issue about which little is known theoretically (Rambau, 2003). Using the results of our paper, it is now possible to give a definite answer to the question of the existence of a triangulation of a hexahedron defined by its eight vertices that respect a given diagonal pattern.

## Acknowledgments

This research is supported by the European Research Council (project HEXTREME, ERC-2015-AdG-694020).

## A Decomposition graphs

We give in this appendix all 174 edge-colored graphs that correpond to combinatorial triangulations fot eh hexahedron that we identified in this work.

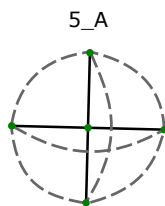


Figure 10: The unique decomposition graph of a hexahedron into 5 tetrahedra.

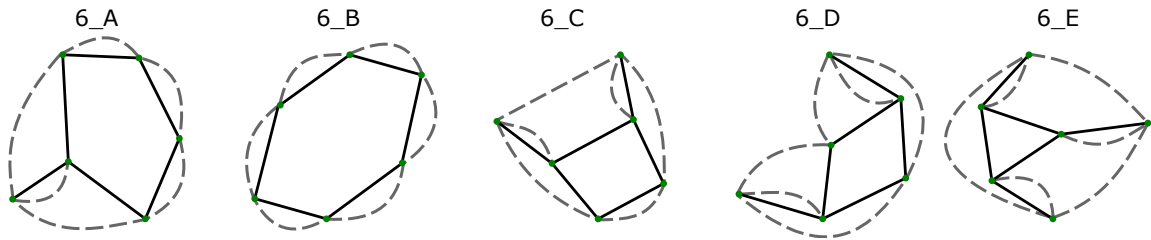


Figure 11: The 5 decomposition graphs of a hexahedron into 6 tetrahedra.

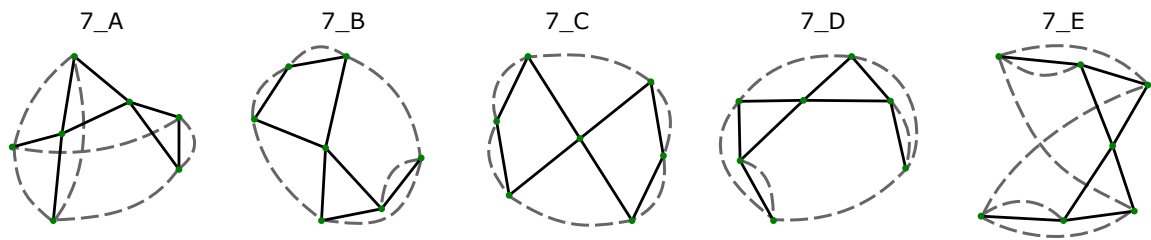


Figure 12: The 5 decomposition graphs of a hexahedron into 7 tetrahedra.

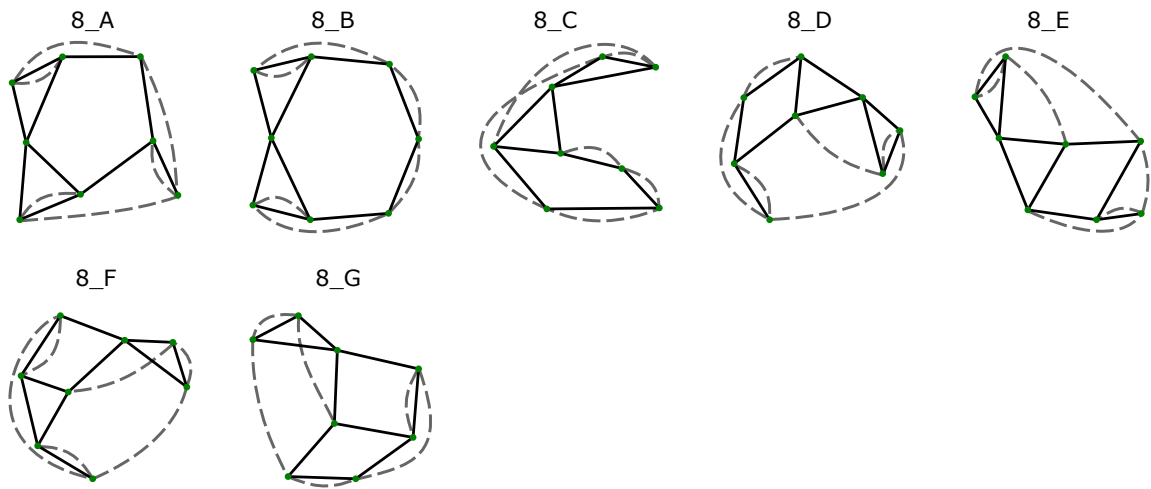


Figure 13: The 7 decomposition patterns of a hexahedron into 8 tetrahedra.

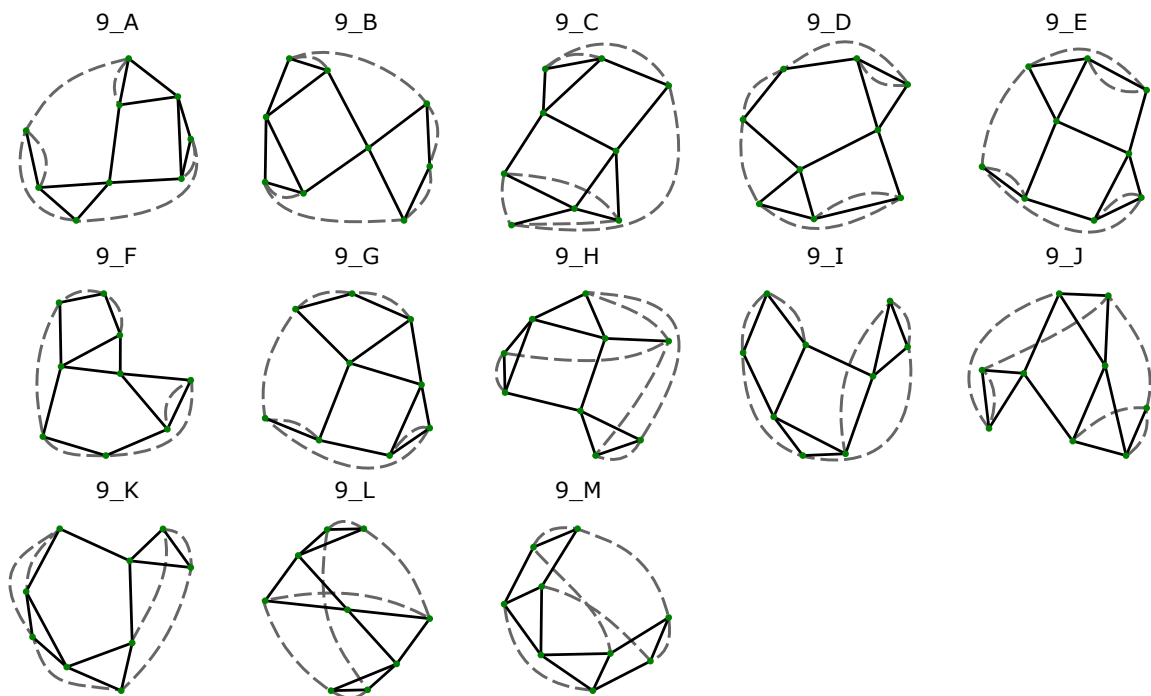


Figure 14: The 13 decomposition graphs of a hexahedron into 9 tetrahedra.



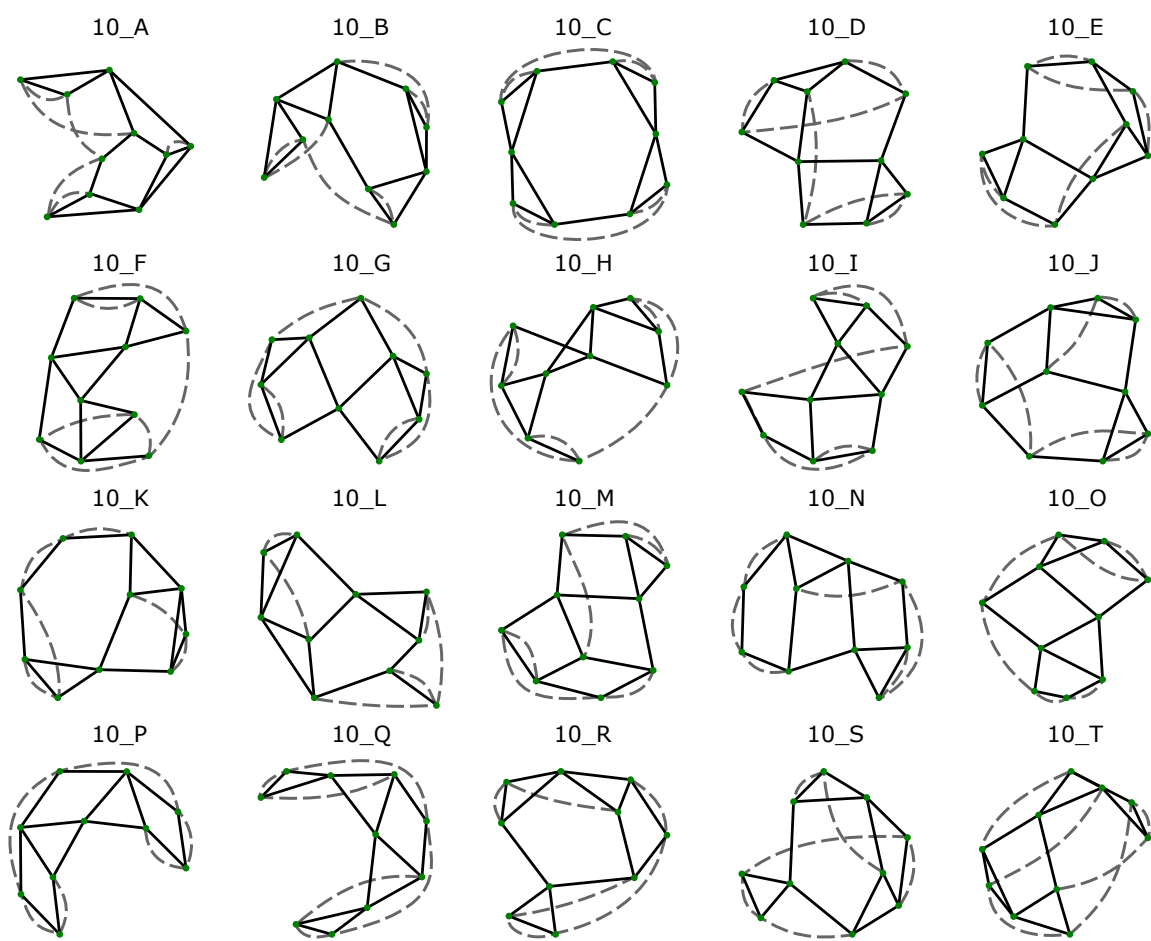


Figure 15: The 20 decomposition graphs of a hexahedron into 10 tetrahedra.

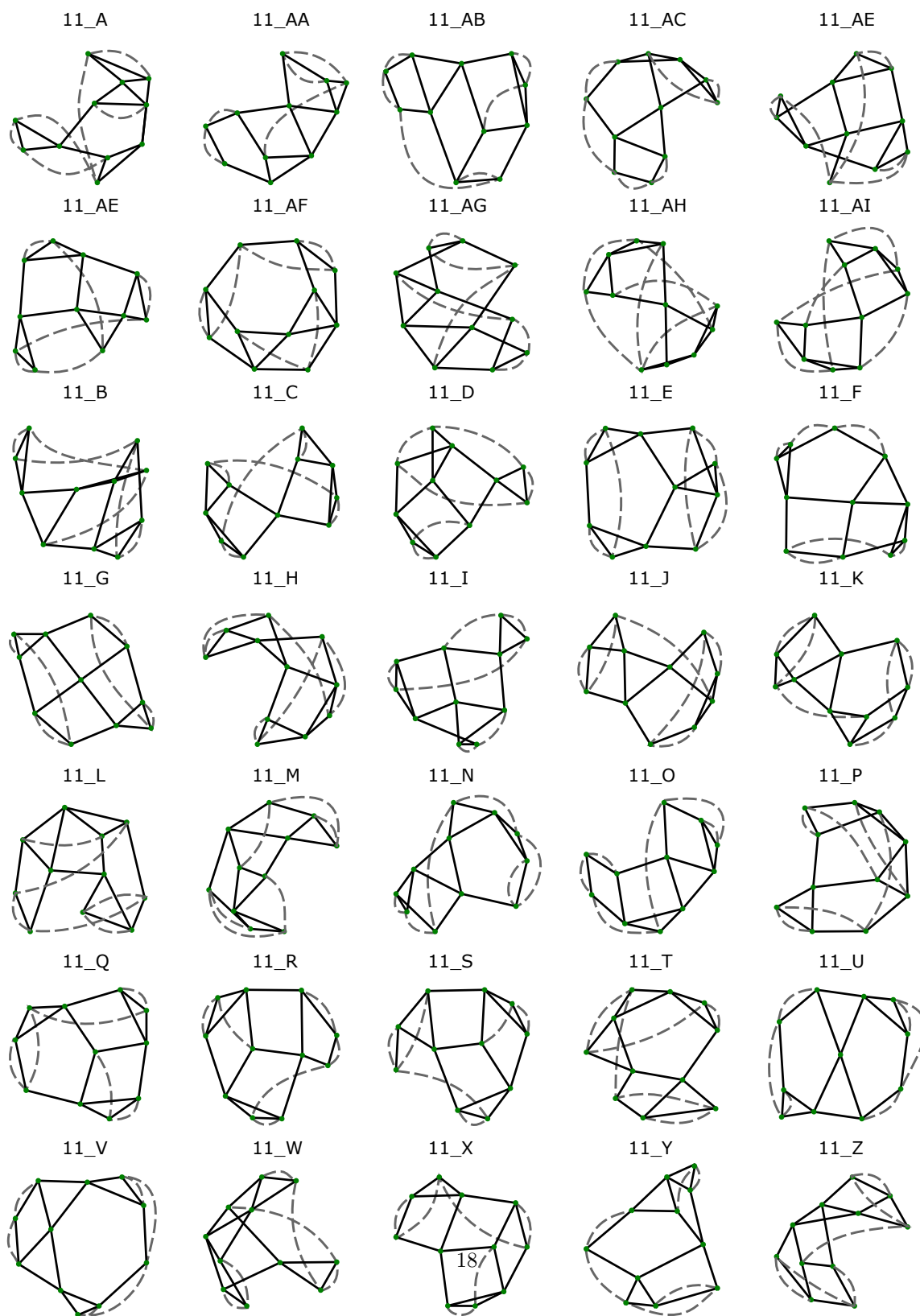


Figure 16: The 35 decomposition graphs of a hexahedron into 11 tetrahedra.

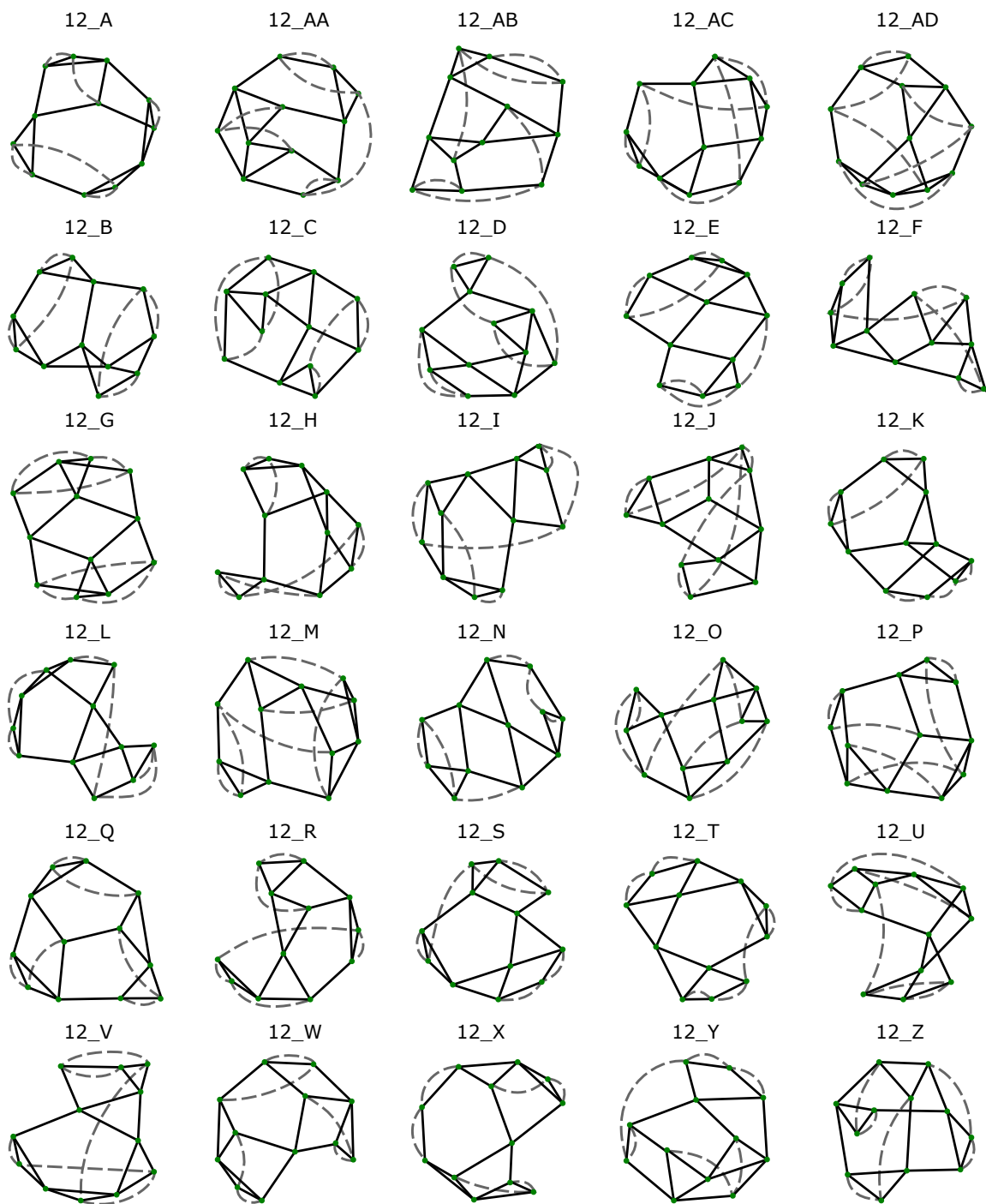


Figure 17: The 30 decomposition graphs of a hexahedron into 12 tetrahedra.

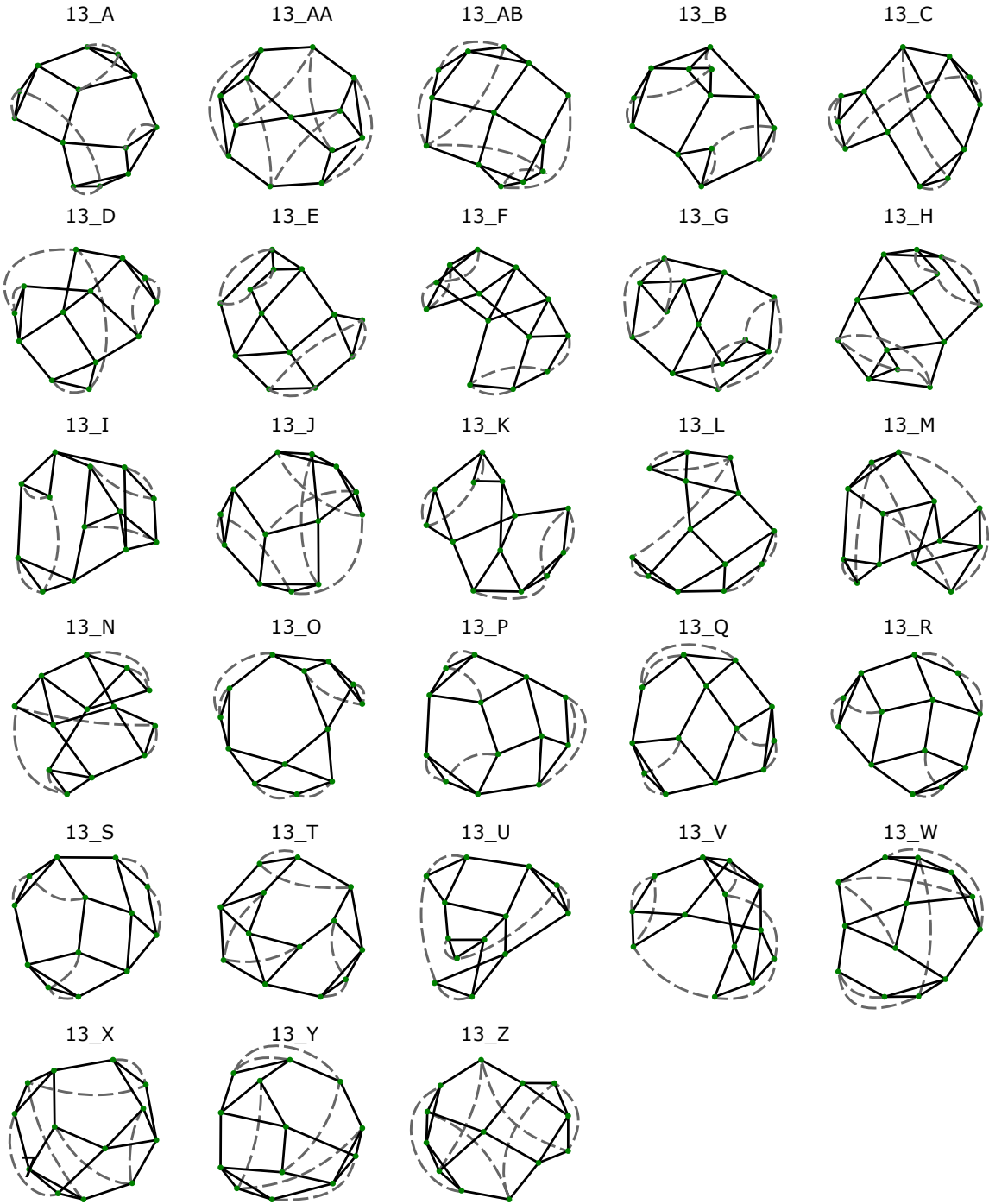


Figure 18: The 28 decomposition graphs of a hexahedron into 13 tetrahedra.

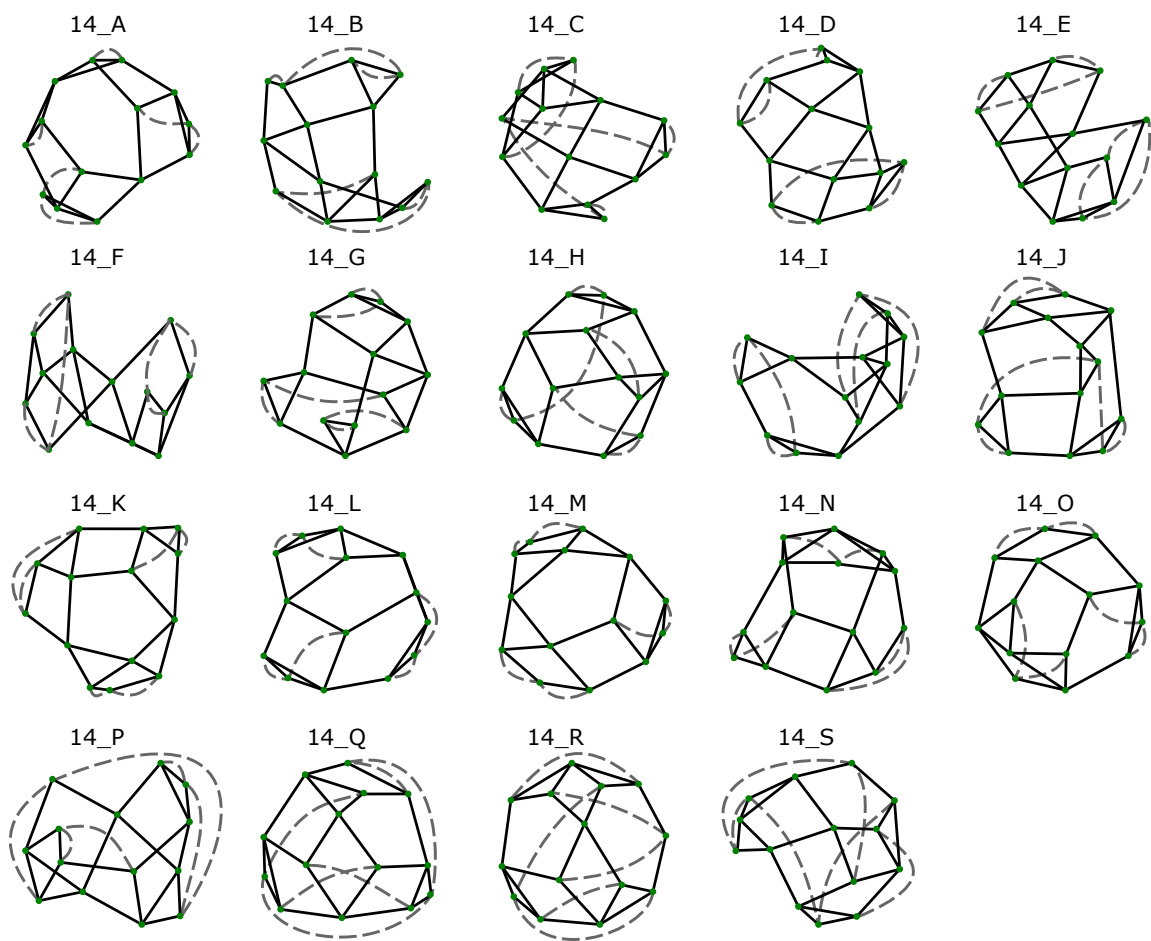


Figure 19: The 19 decomposition graphs of a hexahedron into 14 tetrahedra.

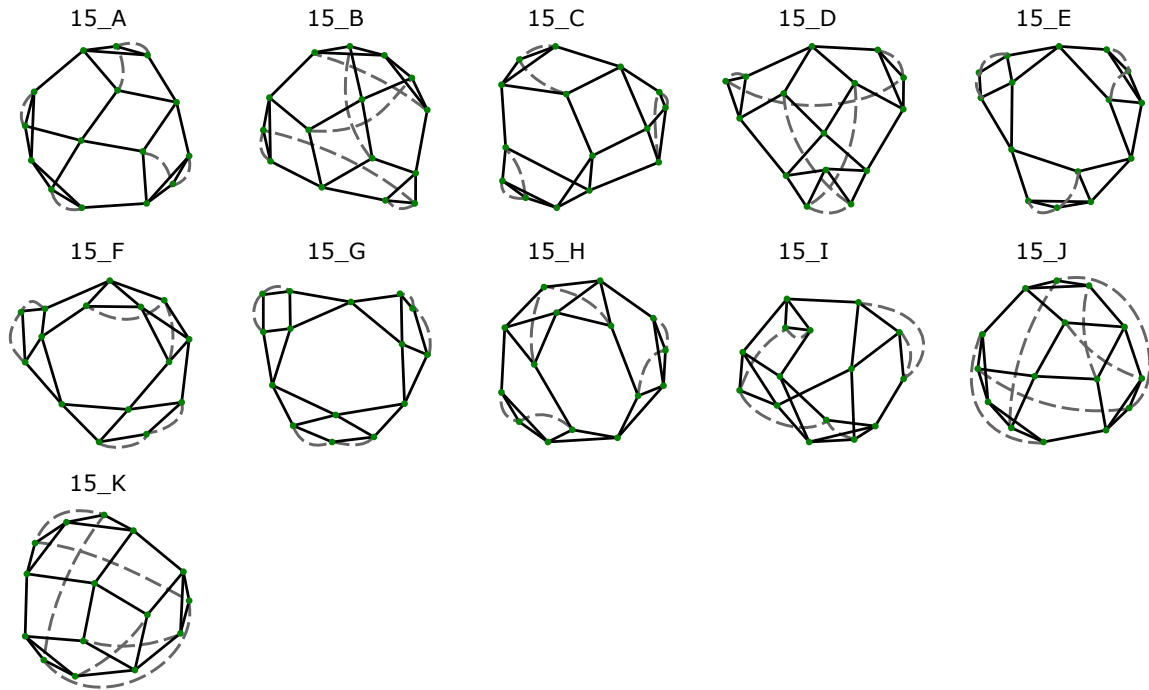


Figure 20: The 11 decomposition graphs of a hexahedron into 15 tetrahedra.

## References

- T. C. Baudouin, J.-F. Remacle, E. Marchandise, F. Henrotte, and C. Geuzaine. A frontal approach to hex-dominant mesh generation. *Advanced Modeling and Simulation in Engineering Sciences*, 1(1):1, 2014. URL <http://amses-journal.springeropen.com/articles/10.1186/2213-7467-1-8>.
- A. Botella, B. Levy, and G. Caumon. Indirect unstructured hex-dominant mesh generation using tetrahedra recombination. *Computational Geosciences*, 20(3):437–451, June 2016. ISSN 1420-0597, 1573-1499. doi: 10.1007/s10596-015-9484-9. URL <http://link.springer.com/10.1007/s10596-015-9484-9>.
- J. A. De Loera, J. Rambau, and F. Santos. *Triangulations: structures for algorithms and applications*. Number v. 25 in Algorithms and computation in mathematics. Springer, Berlin ; New York, 2010. ISBN 978-3-642-12970-4. OCLC: ocn646114288.
- H. Edelsbrunner and E. P. Mücke. Simulation of simplicity: a technique to cope with degenerate cases in geometric algorithms. *ACM Transactions on Graphics*, 9(1):66–104, Jan. 1990. ISSN 07300301. doi: 10.1145/77635.77639. URL <http://portal.acm.org/citation.cfm?doid=77635.77639>.
- H. Edelsbrunner, F. Preparata, and D. West. Tetrahedrizing point sets in three dimensions. *Journal*

- of Symbolic Computation*, 10(3-4):335–347, 1990. ISSN 07477171. doi: 10.1016/S0747-7171(08)80068-5. URL <http://linkinghub.elsevier.com/retrieve/pii/S0747717108800685>.
- J. Huang, Y. Tong, H. Wei, and H. Bao. Boundary aligned smooth 3d cross-frame field. page 1. ACM Press, 2011. ISBN 978-1-4503-0807-6. doi: 10.1145/2024156.2024177.
- B. Levy and Y. Liu.  $L_p$  Centroidal Voronoi Tessellation and its applications. *ACM Transactions on Graphics*, 29(4):1, July 2010. ISSN 07300301. doi: 10.1145/1778765.1778856. URL <http://portal.acm.org/citation.cfm?doid=1778765.1778856>.
- B. D. McKay and A. Piperno. Practical graph isomorphism, II. *Journal of Symbolic Computation*, 60:94–112, Jan. 2014. ISSN 07477171. doi: 10.1016/j.jsc.2013.09.003. URL <http://linkinghub.elsevier.com/retrieve/pii/S0747717113001193>.
- S. Meshkat and D. Talmor. Generating a mixed mesh of hexahedra, pentahedra and tetrahedra from an underlying tetrahedral mesh. *International Journal for Numerical Methods in Engineering*, 49(1-2):17–30, Sept. 2000. ISSN 0029-5981, 1097-0207. doi: 10.1002/1097-0207(20000910/20)49:1/2<17::AID-NME920>3.0.CO;2-U. URL <http://doi.wiley.com/10.1002/1097-0207%2820000910/20%2949%3A1/2%3C17%3A%3AAID-NME920%3E3.O.CO%3B2-U>.
- J. Pellerin, A. Johnen, and J.-F. Remacle. Identifying combinations of tetrahedra into hexahedra: a vertex based strategy. *Procedia Engineering*, 203:2–13, 2017. doi: 10.1016/j.proeng.2017.09.779. Proceedings of the 26th International Meshing Roundtable, Barcelona, Spain.
- J. Rambau. On a generalization of schönhardt’s polyhedron. *Combinatorial and computational geometry*, 52:510–516, 2003. doi: 10.1.1.171.136.
- F. Ruskey. Combinatorial generation. *Preliminary working draft. University of Victoria, Victoria, BC, Canada*, 11:20, 2003. URL <http://www.1stworks.com/ref/RuskeyCombGen.pdf>.
- D. Sokolov, N. Ray, L. Untereiner, and B. Levy. Hexahedral-Dominant Meshing. *ACM Transactions on Graphics*, 35(5):1–23, June 2016. ISSN 07300301. doi: 10.1145/2930662. URL <http://dl.acm.org/citation.cfm?doid=2965650.2930662>.
- S. Yamakawa and K. Shimada. Fully-automated hex-dominant mesh generation with directionality control via packing rectangular solid cells. *International journal for numerical methods in engineering*, 57(15):2099–2129, 2003. URL <http://onlinelibrary.wiley.com/doi/10.1002/nme.754/full>.